Zbigniew CZAJA[1], Michał KOWALEWSKI[1]

Gdansk University of Technology, Faculty of Electronics, Telecommunications and Informatics (1)

doi:10.15199/48.2017.10.14

A compact smart sensor based on a neural classifier for objects modeled by Beaunier's model

***Abstract**. A new solution of a smart microcontroller sensor based on a simple direct sensor-microcontroller interface for technical objects modeled by two-terminal networks and by the Beaunier's model of anticorrosion coating is proposed. The tested object is stimulated by a square pulse and its time voltage response is sampled four times by the internal ADC of microcontroller. A neural classifier based on measurement data classifies the tested object to a given degradation stage.*

***Streszczenie.** Przedstawiono nowe rozwiązanie inteligentnego czujnika opartego na bezpośrednim interfejsie mikrokontroler-czujnik dla obiektów technicznych modelowanych dwójnikami i modelem Beauniera dla powłok antykorozyjnych. Testowany obiekt jest pobudzany impulsem prostokątnym, a jego odpowiedź próbkowana cztery razy przez wewnętrzny przetwornik A/C mikrokontrolera. Klasyfikator neuronowy bazując na wynikach pomiarowych dokonuje klasyfikacji testowanego obiektu do danego etapu degradacji (**Inteligentny kompaktowy czujnik oparty na klasyfikatorze neuronowym dla obiektów modelowanych modelem Beauniera**).*

Keywords: smart sensor, microcontrollers, anticorrosion coating, neural classifiers.
Słowa kluczowe: inteligentne czujniki, mikrokontrolery, powłoki antykorozyjne, klasyfikatory neuronowe.

Introduction

Generally, modern smart sensors integrate analog or digital sensors with conditioning circuits (input circuitries) with communication interfaces, where data processing, data storing and communication control are made by microcontrollers (Fig. 1). Thus, the physical variables of a monitored environment, technical objects and processes are measured, processed and next send to the wireless network by a smart sensor.

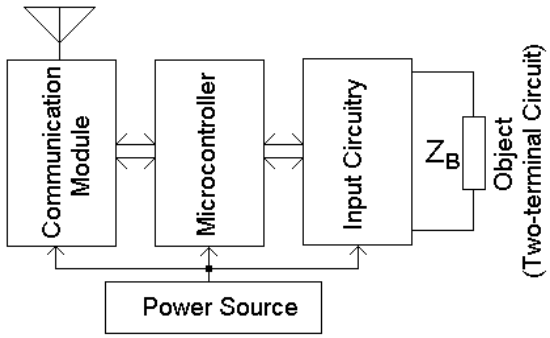

Fig.1. A typical structure of the smart sensor controlled by a microcontroller for objects modeled by two-terminal networks

One of these technical objects is an anticorrosion coating. It can be modeled by a two-terminal network based on the Beaunier's model [1,2]. Thank to such modeling, we can simulate these objects using well-developed tools and methods designed for electrical circuits.

A smart sensor is either battery powered or fed by a power obtained with a harvesting technique. Therefore, it should be designed as an energy-efficient data acquisition system.

Hence, we propose a new solution of a smart microcontroller sensor. It is based on a simple direct sensor-microcontroller interface for objects modeled by two-terminal networks, a simple measurement procedure and a neural classifier used to process and classify the measurement data. The neural classifier is especially useful for dispersed data obtained from a low accuracy microcontroller measurement system working e.g. in a difficult noisy environment. The efficiency of different versions of a minimum distance classifier was also compared.

A model of the tested object

As mentioned earlier, the Beaunier's model of an anticorrosion coating, presented in Fig. 2, has been chosen.

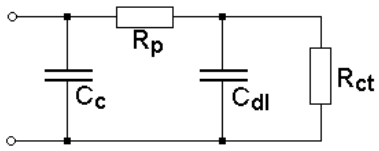

Fig.2. A tested object modeled by a two-terminal network based on the Beaunier's equivalent circuit of an anticorrosion coating

This four-parameter model represents an anticorrosion coating in its early stage of degradation, i.e. the first stage of under-film corrosion [3]. We can distinguish five degradation stages of anticorrosion coating, starting from the nominal stage A, through under-paint corrosion stages B-D, up to the stage E, when the coating is delaminated and penetrated by water [1,2]. The values of parameters of the model for these stages are presented in Table 1.

Table 1. Parameters of anticorrosion coating in different stages of degradation [1,2]

Object	R_p	R_{ct}	C_c	C_{dl}
Stage A	100 GΩ	100 GΩ	10 pF	100 pF
Stage B	10 GΩ	10 GΩ	100 pF	1 nF
Stage C	10 GΩ	1 GΩ	1 nF	10 nF
Stage D	1 GΩ	0.1 GΩ	1 nF	100 nF
Stage E	1 GΩ	0.1 GΩ	1 nF	1 μF

The smart sensor structure

An example of the smart sensor structure is shown in Fig. 3. In the paper we focus only on the measurement part of the sensor, hence the communication module and the power source are omitted. We show only a minimal set of elements needed by the measurement method. The sensor consists of an 8-bit ATxmega32A4 microcontroller [4], an inverting buffer built with IRF7105 [5], a reference resistor R_r and a buffer. The chosen microcontroller performs the following functions:

- generates a signal stimulating the tested object,
- samples the voltage response of the object,
- classifies a stage of the object with the use of a classifier.

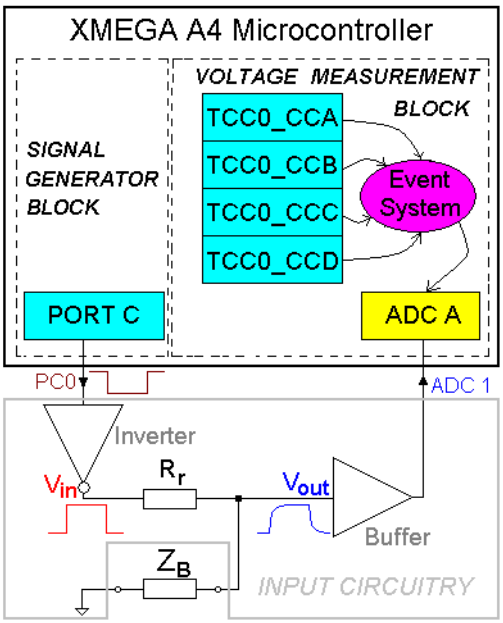

Fig.3. A structure of the measurement part of smart sensor based on an ATxmaga32A4 microcontroller

In the presented solution we propose to fully use the extensive hardware functionality of a 16-bit Timer/Counter TC0 and a 12-bit ADC. Each of these peripherals have four channels, which can be synchronized by an event system. Therefore, the voltage response is sampled four times. It simplifies the measurement algorithm and improves the measurement accuracy.

An amplitude of the stimulating pulse V_{in} is set to 2.5 V. It follows from the fact that a reference voltage V_{ref} of the ADC is equal to $V_{cc} - V_D$ (V_{cc} = 3.3 V, $V_D \approx$ 0.7 V).

The comparisons in channels A, B, C and D of the TC0 determine the moments of voltage sample conversions in channels 0, 1, 2 and 3 of the ADC, respectively. The inverter eliminates a negative effect of a varying impedance of the output pin PC0 [7] and the buffer provides a large input impedance of the input circuitry.

The measurement procedure

The timing of the measurement procedure, similar to that presented in [6], is shown in Fig. 4. The stimulating pulse V_{in}, the time responses V_{out} of the object for all degradation stages and four sample moments are plotted in the figure.

The algorithm of this procedure is partly implemented in the program code of the microcontroller (Fig. 5), and partly in the microcontroller hardware configuration (i.e., in its peripheral devices) (Fig. 6). Hence, a description of the measurement procedure requires simultaneous analysis of Figures 4, 5 and 6. The steps of the algorithm are marked in the figures in the form of numbers in circles.

In the first step the TC0 is started and the stimulating pulse is generated. Also, four sample moments t_1, t_2, t_3 and t_4 are set, where a time interval between samples t_s = 131.072 ms. At the end of this step the *end_conv* variable is set. It is used to synchronize the software with the hardware of the microcontroller.

As it is seen in Fig. 6, the ADC A, without a participation of software, samples four times the time response at the ADC 1 input. A match in the TCC0_CCA (counting the time t_1 – the second step) triggers the first AD conversion on the CH0, a match in the TCC0_CCB (counting the time t_2 – the third step) triggers the second one on the CH1, a match in the TCC0_CCC (counting the time t_3 – the fourth step) triggers the third one on the CH2, and a match in the TCC0_CCD (counting the time t_4– the fifth step) triggers the fourth one on the CH3. When the ADC conversion on the channel CH3 is completed, an interrupt is generated. During its service the TC0 is stopped, generation of the pulse is ended (the sixth step) and the *end_conv* flag is cleared, which informs the main function that all voltage measurements have been completed.

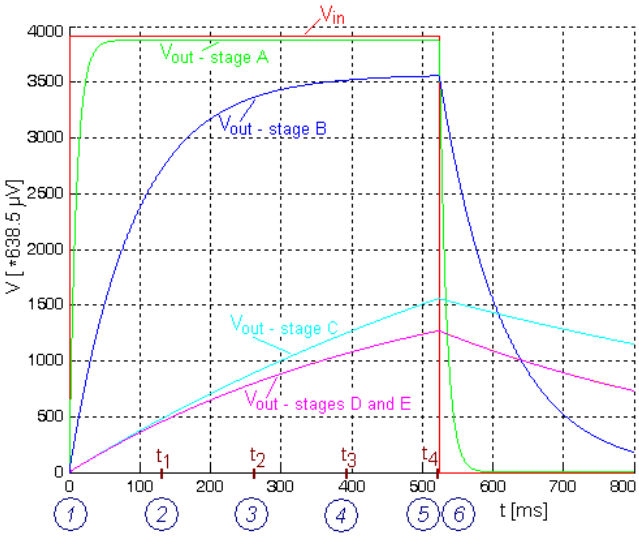

Fig.4. The timing of the measurement procedure, R_r = 1 GΩ

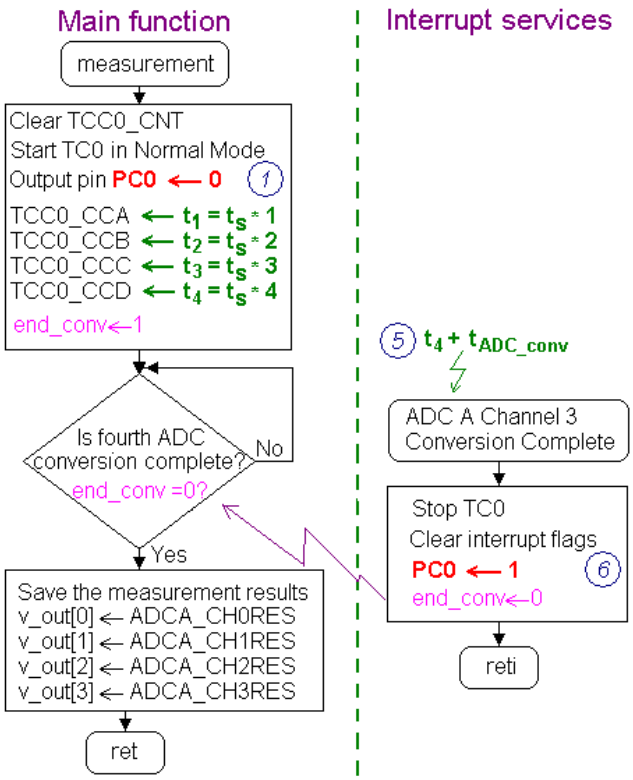

Fig.5. A flowchart of the algorithm of the measurement procedure

The results of AD conversions are placed in the ADC A result registers: CH0RES, CH1RES, CH2RES and CH3RES. At the end of the main function these values are saved in the *v_out* table containing four 16-bit variables.

In the next step the measured samples of the response are used by the classifier in order to determine a stage of degradation of the tested object.

MOST WIEDZY Downloaded from mostwiedzy.pl

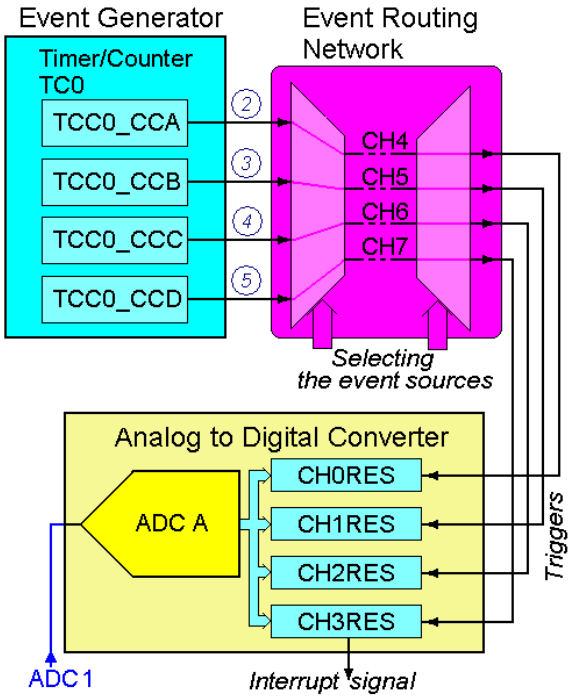

Fig.6. A block scheme of the sensor part configured from peripheral devices of the ATXmega32A4 microcontroller

Data preparation

Simulation of the model of the anticorrosion coating performed for different stages of degradation have shown that using the selected measurement method we are not able to distinguish stages D and E. Therefore, further studies are focused exclusively on the distinction of stages from A to D.

It should be noticed, that based on the values of parameters given in Table 1 we are able to calculate the coordinates of only 4 points corresponding to the considered stages in a 4-dimensional input space with the coordinates: $u(t_1)$, $u(t_2)$, $u(t_3)$ and $u(t_4)$. However, it is important to examine the behavior of the coating in transitional stages, when values of parameters differ from those given in the table. This will also be useful when checking the effectiveness of the classifiers, which in practice should operate on real measurement results and should have sufficient generalization capabilities. Hence, it was assumed that the values of parameters change either linearly or logarithmically (Fig. 7), depending on the neighboring parameter values given in Table 1.

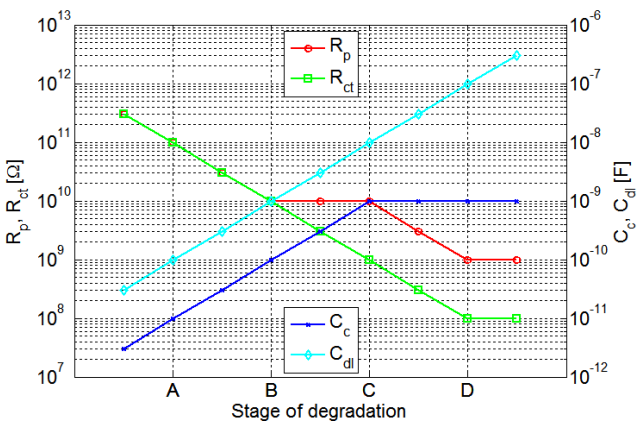

Fig.7. Values of the anticorrosion coating parameters in different stages of degradation

In the next step four test sets (for stages from A to D), containing 1000 signatures each, were generated. A random dispersion of values of all parameters at intervals corresponding to individual stages was assumed. Each test set is a cluster of data in a 4-dimensional input space. All clusters in a 2-dimensional space with the coordinates $u(t_1)$ and $u(t_4)$ are shown in Fig. 8. The points marked with circles correspond to the values obtained from Table 1 and a broken curve, marked with black, corresponds to the values of coating parameters obtained from Fig. 7.

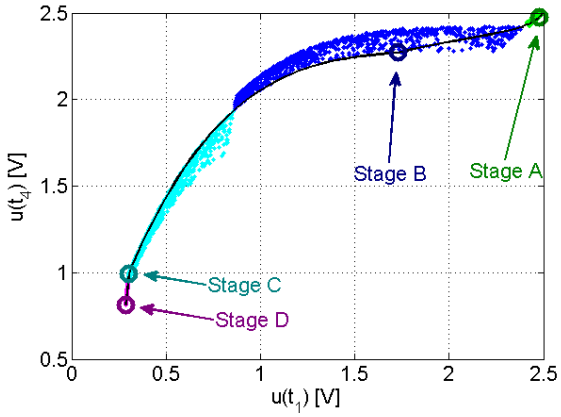

Fig.8. Test sets in a 2-dimensional input space

Using typical classifiers

The problem of classification of a stage of anticorrosion coating can be treated as a dictionary method of detecting catastrophic faults in analog electronic circuits. In the simplest words, the method depends on using a Minimum Distance (MD) classifier on a set of signatures of faults. For that purpose no further data processing is required. The efficiency of this classification method is weak when we take into account tolerances of parameters. In the case of anticorrosion coating the classification error is equal to 17.7%. To increase the efficiency of the classifier, the signatures of stages were assumed to be the mean positions of clusters. These points are marked as squares in Fig. 9, which shows the data clusters in a 3-dimensional space with the coordinates $u(t_2)$, $u(t_3)$ and $u(t_4)$. In this case, the classification error on data sets is reduced to 12.3%, which is still not acceptable.

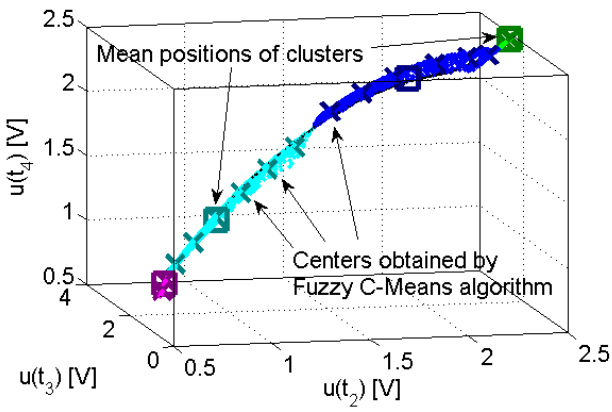

Fig.9. Test sets in a 3-dimensional input space with marked centers of different versions of the minimum distance classifier.

One solution in classification of signatures of stretched clusters in fault dictionary methods is increasing the number of centers assigned to classes. This method increases also

MOST WIEDZY Downloaded from mostwiedzy.pl

the number of calculations, but guarantees a better fit to the shapes of data clusters. We used the Fuzzy C-Means (FCM) clustering algorithm. Due to different structures of clusters, different numbers of centers were also assumed: 2 for stages A, D and 6 for stages B, C. These centers, marked 'x', are shown in Fig. 9. Consequently, increasing the number of centers in the MD classifier reduced the classification error to 0.6%.

A specialized neural classifier with TCSB functions

The previous research on diagnosis parametric faults of analog electronic circuits performed by the authors proved a high effectiveness of the specialized neural network with Two-Center Basis Functions (TCB Functions) [7-9]. For the purpose of this study a simplified version of the TCB function was used. The new function radially transforms the space around a line segment connecting two centers $\mathbf{c}^{(1)}$ and $\mathbf{c}^{(2)}$ with the equation:

$$y(\mathbf{x}) = \left(\frac{\left\| \mathbf{x} - \mathbf{w}(\mathbf{x}) \right\|}{s(\mathbf{x})} \right)^2, \qquad (1)$$

where: $s(\mathbf{x})$ is a *scaling function* and $\mathbf{w}(\mathbf{x})$ are *center functions* depending on the coordinates of centers. In order to decrease the computational complexity, in respect to the previous versions, the exponential function was eliminated from the equation. The method of transformation of the space is now square - hence the function's name is Two-Center Square Basis (TCSB). An example of the TCSB function shape in a 2-dimensional space with the coordinates x_1 and x_2 in arbitrary units (au) is shown in Fig. 10. The coordinates of centers are: $\mathbf{c}^{(1)}$ = (1, 1), $\mathbf{c}^{(2)}$ = (2, 2).

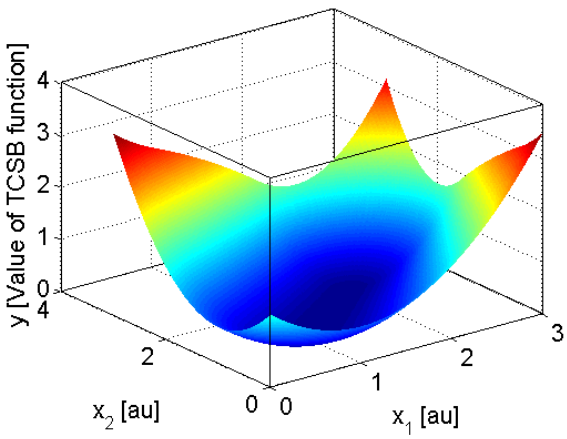

Fig.10. An example of the TCSB function shape in a 2-dimensional input space with the coordinates x_1 and x_2 (au – arbitrary unit)

The neural classifier with 4 TCSB functions assigned to stages from A to D was constructed. For the purpose of calculating centers of these functions, the curves shown in Fig. 7 were taken into account. Five selected centers of TCSB functions correspond to the values of parameters for the middle positions between predefined stages. Classifying a stage of the anticorrosion coating is the same as in the MD classifier, except that we do not compare the distances from the measurement signature to all centers, but the squares of the distances from the measurement signature to the segments connecting centers of TCSB functions. In both cases we select a center or a function that is closest to the measurement signature. Each center or function is assigned to a particular stage of the coating and the minimum distance value strictly indicates that stage.

In the simulation all signatures contained in the test data sets were correctly classified with the TCSB function classifier.

Table 2 lists the basic parameters of analyzed classifiers. The times of calculations for the MD classifier with the FCM clustering algorithm and the TCSB function classifier are comparable. However, there is a noticeable increase in the computational complexity per center in the TCSB function classifier. This disadvantage is compensated by a lower demand for the number of centers required to cover clusters of data, because the activation area for the TCSB function is much larger than that for a single center in the MD classifier.

Table 2. Comparison of classifiers

Classifier	Number of centers	Time of calculations [time arbitrary unit]		Classification error [%]
		total	per center	
MD	4	7	1.8	17.7
MD (mean)				12.3
MD (FCM)	16	61	3.8	0.6
TCSB	5	52	10.4	0.0

Conclusions

A compact smart sensor presented in this paper can be used for diagnosis of technical objects modeled by a two-terminal network, e.g. anticorrosion coatings. With only two voltage buffers and a reference resistor we can excite an object with a square voltage pulse and measure its response. Four voltage samples are used by the classifier to determine a degradation stage of the anticorrosion coating. Using a neural classifier with TCSB functions provides a better fit to the shape of complex structures of data clusters, than obtained by using simple classifiers based on a minimum distance.

***Autors**: dr hab. inż. Zbigniew Czaja, dr inż. Michał Kowalewski, Gdansk University of Technology, Faculty of Electronics, Telecommunications and Informatics, Department of Metrology and Optoelectronics, ul. G. Narutowicza 11/12, 80-233 Gdańsk, E-mail: zbczaja@pg.gda.pl, Michal.Kowalewski@eti.pg.gda.pl.*

REFERENCES

[1] Niedostatkiewicz M., Lentka G., Test frequencies selection criteria for parameter identification of anticorrosion coating using bilinear transformation, *16th IMEKO TC4 Symposium*, Florence, Italy, (2008)
[2] Niedostatkiewicz M., Lentka G., Frequencies selection for accelerated CNLS parameter identification of anticorrosion coatings,
[3] Mansfeld F., Kendig M.W., Tsai C.H., Evaluation of Corrosion Behavior of Coated Metals with AC Impedance Measurements, *Corrosion* 38 (1982), 478-485
[4] Atmel Corporation, Atmel AVR XMEGA AU Manual, (2012), PDF file available from: www.atmel.com
[5] International Rectifier, IRF7105 HEXFET Power MOSFET, El Segundo, CA, USA, (2003), PDF file available: http://www.irf.com
[6] Czaja Z., A microcontroller system for measurement of three independent components in impedance sensors using a single square pulse, *Sensors and Actuators A*, 173, (2013), 284-292
[7] Kowalewski M., Zielonko R., A New Two-center Ellipsoidal Basis Function Neural Network for Fault Diagnosis of Analog Electronic Circuits, *Proc. of the 2nd Int. Conf. on Information Technology ICIT 2010*, Gdańsk, (2010), 143-146
[8] Czaja Z., Kowalewski M., An Application of TCRBF Neural Network in Multi-node Fault Diagnosis Method, *IMEKO XIX World Congress, Lisbon, Portugal*, (2009), 503 – 508
[9] Czaja Z., Kowalewski M., A New Method for Diagnosis of Analog Parts in Electronic Embedded Systems with Two Center Radial Basis Function Neural Networks, *16th IMEKO TC4 Symposium*, Florence, Italy, (2008), 743-748

MOST WIEDZY Downloaded from mostwiedzy.pl